Fit αβ T-cell receptor suppresses leukemogenesis of Pten-deficient thymocytes

Stéphanie Gon,[1*] Marie Loosveld,[1,2*] Thomas Crouzet,[1] Delphine Potier,[1] Mélanie Bonnet,[1] Stéphanie O. Morin,[3] Gérard Michel,[4] Norbert Vey,[3,5] Jacques A. Nunès,[3] Bernard Malissen,[1] Romain Roncagalli,[1] Bertrand Nadel,[1] and Dominique Payet-Bornet[1]

[1]Aix-Marseille Université, CNRS, INSERM, CIML; [2]APHM, Hôpital La Timone, Laboratoire d'Hématologie; [3]Aix-Marseille Université, CNRS, INSERM, Institut Paoli-Calmettes, CRCM; [4]APHM, Hôpital La Timone, Service d'Hématologie et d'Oncologie Pédiatrique and [5]Institut Paoli-Calmettes, Hematology Department, Marseille, France

**These authors contributed equally to this work.*

 doi:10.3324/haematol.2018.188359

Received: January 11, 2018.

Accepted: March 15, 2018.

Pre-published: March 22, 2018.

Correspondence: payet@ciml.univ-mrs.fr or nadel@ciml.univ-mrs.fr

Supplementary data for

Fit αβ T-Cell Receptor suppresses leukemogenesis of Pten-deficient thymocytes.

This PDF file includes:

Supplementary Materials & Methods

Mice

Immunodeficient NOD.Cg-*Prkdc* ^{scid} *Il2g* ^{tm1Wji} /SzJ mice (abbreviated NSG) used for xenotransplantation are from Charles River. C57BL/6J mice (denoted WT in this manuscript) and BALB/C mice are from Janvier labs. B6.129S7-*Rag1*^{tm1Mom} Tg (TcraTcrb) 425Cbn (abbreviated [OT-II x Rag1$^{-/-}$]) are from Taconic. Conditional Pten$^{flox/flox}$ mice [1] were obtained from European Mouse Mutant Archives (EMMA). ROSA26-YFP reporter mice [2] and Ubiquitin-CreERT2 mice (B6.Cg-Tg(UBC-cre/ERT2)1Ejb/J, strain 8085) were purchased from The Jackson Laboratory. Rag1$^{-/-}$, CD4-Cre [3], Cdkn2a$^{-/-}$ [4] and H-Y transgenic mice[5] were bred and maintained in CIML animal facilities.

Cdkn2a$^{-/-}$ T-ALL mouse model

Cdkn2a$^{-/-}$ mice [4] can't be exploited directly as a T-ALL mouse model because they primarily develop skin or liver tumors. Thus, to obtain *Cdkn2a*$^{-/-}$ T-ALL, four-week-old *Cdkn2a*$^{-/-}$ mice were injected intravenously with 5-fluorouracil (150 mg/kg) 5 days prior to sacrifice. Then bone marrow (BM) cells from these mice were collected and co-cultured for 10 days on confluent OP9-DL1

stromal cells in a α-MEM media supplemented with 20% FBS (Hyclone, Thermo Fisher Scientific), 50 µg/ml streptomycin and 50 IU penicillin. Recombinant mouse cytokines FLT3-L (5 ng/mL) and IL-7 (2 ng/mL) (Peprotech, Rock Hill) were added to the culture. After 10 days of co-culture, cells were recovered into 8-12 week-old NSG mice. Mice developed leukemia in around 4 months. Transplantability of tumor was assessed by tail vein injection of 10^6 tumoral cells from a leukemic mouse into NSG mice.

Xenotransplantation

Xenotransplantation was performed as previously described [6]. Briefly primary human leukemia cells from peripheral blood or bone marrow were intravenously injected into tail vein of immunodeficient NSG mice. 1 to 10 × 10^6 cells were injected per mouse. Engraftment was determined by flow cytometric analysis of peripheral blood using antibodies against human CD45 (APC-Cy7) and mouse CD45 (PE) (Supplementary Tables S2 & S3). At first signs of disease, human grafts were harvested from the spleen of NSG mice and were either frozen in 10% DMSO, 90% FCS or injected again in NSG mice (10^6 cells per mouse) to create secondary xenografts. Typically, secondary xenografts were used for *in vitro* assays.

Human and Mouse T cell isolation

Mouse CD4+ T cells were purified from spleens of wild-type or leukemic mice with Dynabeads Untouched Mouse CD4 cells kit (Life Technologies, France) with a cell purity of over 90%. Human CD4+ SP T cells were purified from thymus from healthy donors with Dynabeads Untouched human CD4 cells kit (Life Technologies, France) with a cell purity of over 80%.

Flow cytometry analysis

Single-cell suspensions were stained with conjugated antibodies for 30 min at 4 °C and washed twice with FACS buffer (PBS, 2 % FCS, 1 mM EDTA). Multicolor flow cytometry analysis was performed with FACS Canto II (Becton–Dickinson Pharmingen) and data analyzed with FlowJo software (Tree Star, Ashland). Antibodies, clone numbers, and conjugates of antibodies used for flow cytometry are listed in Supplementary Table S2 (Human antibodies) and Supplementary Table S3 (Mouse antibodies). For mouse TCR Vβ clonotyping, we used the 'Mouse Vβ TCR screening panel' (BD Biosciences).

Immunoblotting.

Antibodies used for immunobloting are listed in Supplementary Table S4. When fluorescent secondary antibodies were used, immunoblots were analyzed using an Odyssey® infrared imaging system (Li-Cor Biosciences). For multiple probing, blots were stripped using Restore western blot stripping buffer (Pierce). Quantification of protein levels was determined after immunoblotting using the ImageJ software.

Real-time Quantitative PCR (RQ-PCR).

RNA was extracted from cells using the column-based system RNAeasy mini kit (Qiagen) according to the manufacturer's instructions. Reverse-transcription was performed with High-capacity cDNA reverse transcription kit (Applied Biosystems), and cDNA was analyzed by real-time PCR (RQ-PCR) on an ABI-PRISM 7500 Fast Real-Time PCR system (Applied Biosystems). PCR reactions were performed in 25 µl of diluted cDNA (10X dilution), 0.3 µmol of each primer and 12.5 µl of

SYBR Green Master Mix (Roche). Oligonucleotides used for RQ-PCR are listed in Supplementary Table S1. All RQ-PCR were performed in duplicate. To allow comparison between samples, transcript quantification was performed after normalization with ABL using the ΔCt method and calculated according to the following formula 2Δ (CtABL-Ctgene).

Supplementary Figures

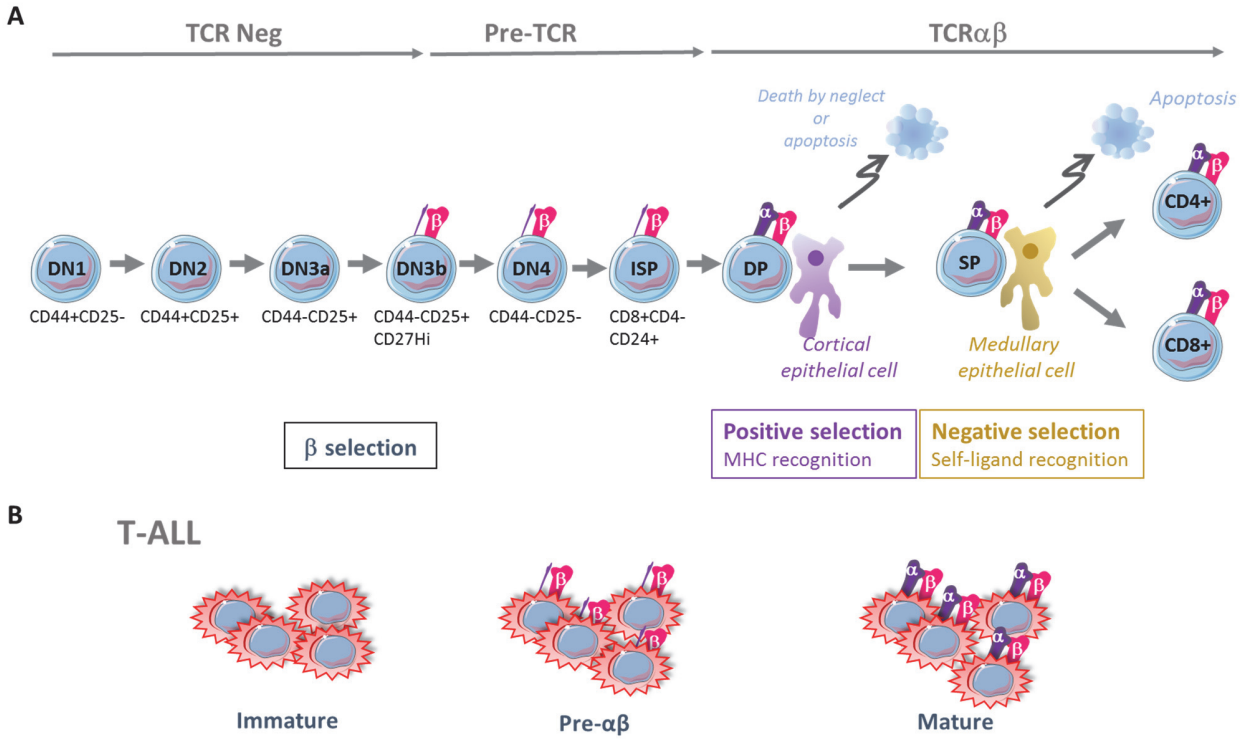

Supplementary Figure S1: Major αβ-T cell differentiation stages and T-ALL counterparts.

(**A**) T-Lymphocytes differentiation occurs in the thymus and can be followed by various surface markers notably CD4 and CD8. In mouse, the early $CD4^{-}CD8^{-}$ double-negative (DN) thymocytes can be further subdivided into 4 distinct differentiation stages (DN1 to DN4). Throughout the gene rearrangement process, thymocytes committed to the αβ lineage undergo various quality controls of their TCR. During the β-selection checkpoint, which occurs at the DN3 stage of differentiation in mouse and the equivalent intermediate $CD4^{+}$ immature single-positive stage (ISP) in human, T-cells that have rearranged a proper TCRβ chain and successfully assembled a surface pre-α/β TCR receptor, are selected to pursue their maturation and initiate TCRα rearrangement. At the double-positive (DP) $CD4^{+}CD8^{+}$ stage, thymocytes which have rearranged a TCRα chain and successfully assembled a surface α/βTCR receptor undergo two additional checkpoints. During the positive selection, thymocytes harboring unfit αβTCR, *i.e.* unable to bind self-peptide -major histocompatibility complex (p-MHC) class I or II molecules with at least a weak affinity, are purged by 'death by neglect'. Conversely, binding MHC with sufficient affinity triggers

survival through TCR signaling, allowing positive selection and lineage commitment into a $CD8^+$ T cell (restricted to MHC-I) or a $CD4^+$ T-cell (restricted to MHC-II) single-positive (SP) thymocyte. SP thymocytes finally migrate to the medulla, and eventually proceed to the negative selection, which eliminates by apoptosis auto-reactive cells bearing TCRs that bind with high affinity to p-MHC complexes. The few thymocytes emerging from these 3 drastic selection processes exit the thymus and reach the pool of peripheral TCRαβ $CD4^+$ or $CD8^+$ T-cells with classical helper and cytotoxic functions.

(**B**) T-ALL mirrors T-Cell ontogeny. Some genetic hits (*e.g. LYL1, TLX1,* and *TAL1*) appear to be mutually exclusive and delineate distinct subgroups, each correlating with a given stage of thymocyte developmental arrest (immature/DN, intermediate/pre-$\alpha\beta$, and mature/TCR$\gamma\delta$ or TCR$\alpha\beta^+$, respectively)[7-9]. By contrast, other deregulations, such as constitutive NOTCH1 activation[10] or inactivation of tumor suppressor genes CDKN2A/p14ARF[11] and PTEN are found in a large proportion of cases and irrespective of subgroups. Most of the deregulations, in any case, are found in various combinations, suggesting the occurrence of multiple oncogenic cooperation pathways.

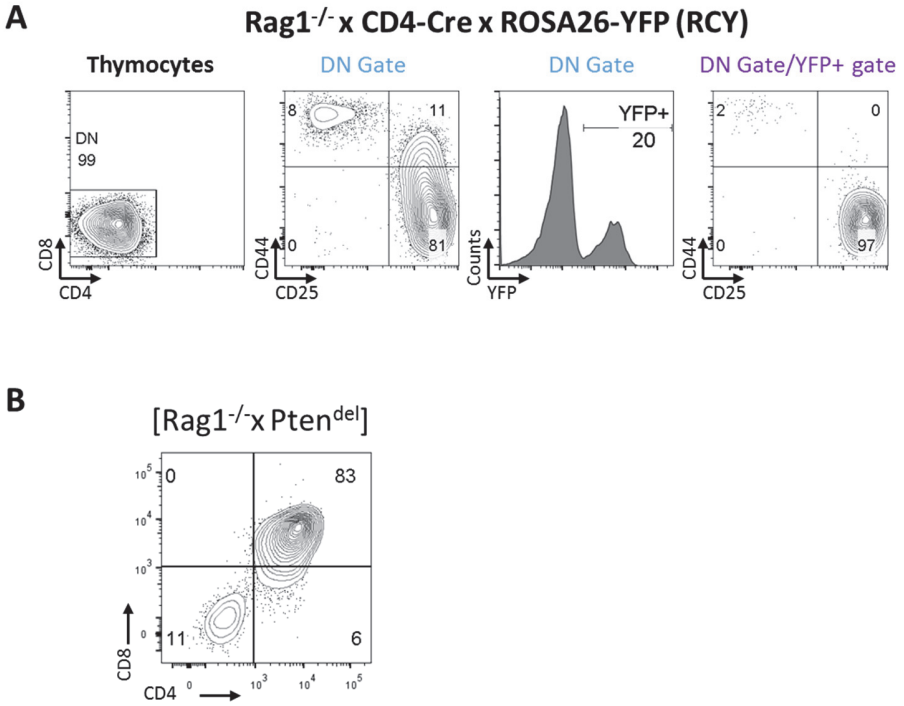

Supplementary Figure S2: Activation of CD4-Cre in Rag1$^{-/-}$ thymocytes. (A) Flow cytometry analysis of CD4, CD8, CD44, CD25 and yellow fluorescent protein (YFP) expression in a typical fate-mapping mice [Rag1$^{-/-}$x CD4-Cre x ROSA26-YFP] (named RCY). In RCY model, Cre recombinase is activated in some DN3 cells (mean % of YFP+ cells is 23.5%; n=6 RCY mice). **(B)** DP [Rag1$^{-/-}$x Pten^{del}] thymocytes are malignant. Flow cytometry analysis of splenocytes from a representative NSG mouse transplanted with 1.10^6 [Rag1$^{-/-}$x Pten^{del}] thymocytes is shown.

Rag-deficient thymocytes are blocked at the DN3 stage, while full activation of CD4-cre transgene occurs later on, at the DP stage [3]. Using RCY fate-mapping mice in which Cre-expressing cells express YFP [2] we observed a leakage of Cre expression during DN3 stage. [Rag1$^{-/-}$ x Pten^{del}] mice presented an enlarged thymus composed mainly of malignant DP CD4$^+$CD8$^+$ T-cells (Fig. 1A & B), here in panel B we demonstrate that these DP cells are malignant as they readily engrafted NSG mice. Of note, Rag1$^{-/-}$ thymocytes are normally arrested at DN3a stage (before β-selection), and should thus not reach DP stage of development; however *Pten* deletion allows to bypass the requirements for IL-7 and β-selection resulting in survival, proliferation and DN to DP differentiation of Rag/Pten deficient thymocytes [12,13].

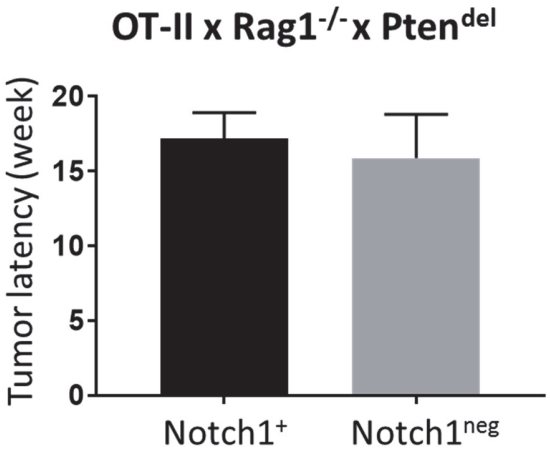

Supplementary Figure S3: Notch1 activation does not impact latency of [OT-II x Rag1$^{-/-}$ x Pten^{del}] tumors. Seven T-LBL generated by [OT-II x Rag1$^{-/-}$ x Pten^{del}] mice were analyzed by immunoblot using an antibody specific for cleaved Notch1. 3 were Notch1 activated (Notch1+) and 4 were Notch1^{neg}. Weeks of survival were plotted, mean values are 17 and 16 weeks for Notch1+ and Notch1^{neg} tumors respectively.

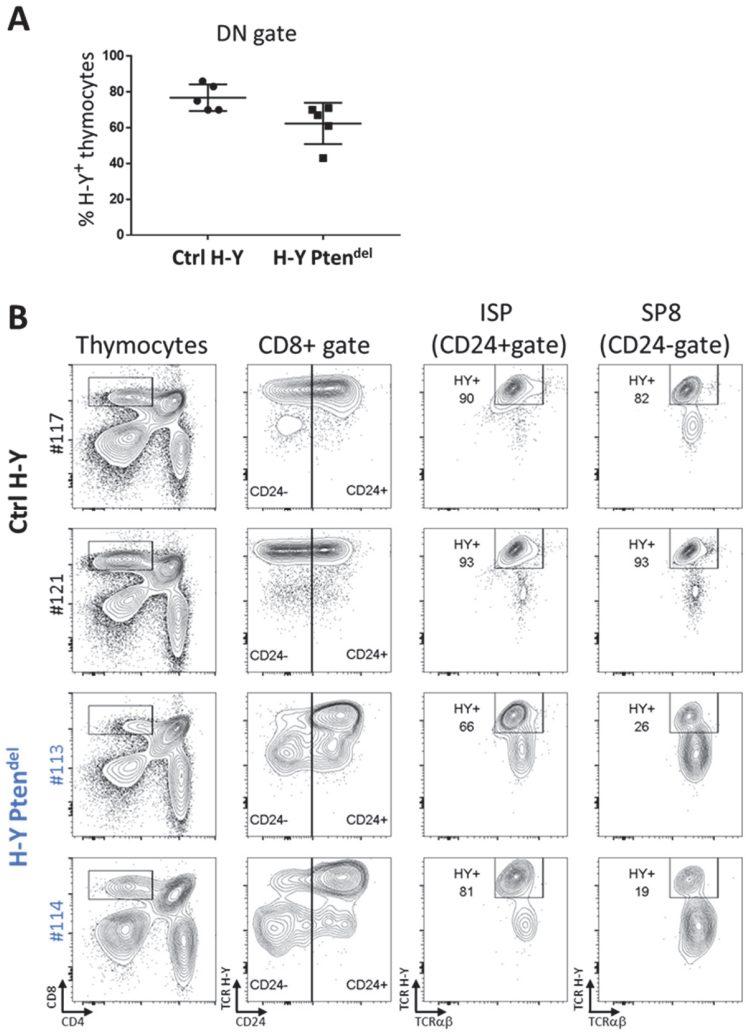

Supplementary figure S4: Elimination of H-Y+ thymocytes occurs at a post β-selection stage. (**A & B**) Analysis of young (4 weeks old) control H-Y and [H-Y x Pten^{del}] female mice. (**A**) Percentages of TCR H-Y+ thymocytes within the CD4$^-$CD8$^-$ (DN) gate. (**B**) Flow cytometry analysis of thymus from 2 representative control H-Y and [H-Y x Pten^{del}] mice. First row: CD4/CD8 expression, SP CD8 cells are gated. Second row: TCR H-Y/CD24 expression within SP CD8 gates; cells were separated according to CD24 expression. CD24^{high} cells correspond to immature SP CD8 cells (ISP) while CD24^{low} to mature SP8 cells. Third and fourth rows show TCR H-Y/TCRαβ expression in ISP and SP8 cells respectively; percentages of H-Y+ cells are indicated.

Due to premature expression of TCRα chain in the H-Y model used in this study, a large amount of DN cells expressing H-Y TCR are generated in the thymus. It has been shown that most of those

cells 1°) were functionally mature, 2°) were not *bona fide* precursors of DP thymocytes, 3°) were misguided γδ lineage cells that express transgenic αβTCR (reviewed in [14-16]). Data in (A) show that percentages of H-Y+ cells in DN gate are mildly impacted in [H-Y x Pten^{del}] female mice. Data in (B) show that most of the SP CD8 cells (both ISP and mature SP8) in control H-Y mice express H-Y TCR. In [H-Y x Pten^{del}] mice the majority of ISP cells express H-Y TCR while most of mature SP8 are TCR H-Y^{neg}, suggesting that the elimination of H-Y+ thymocytes occurs after ISP stage (and consequently after β-selection).

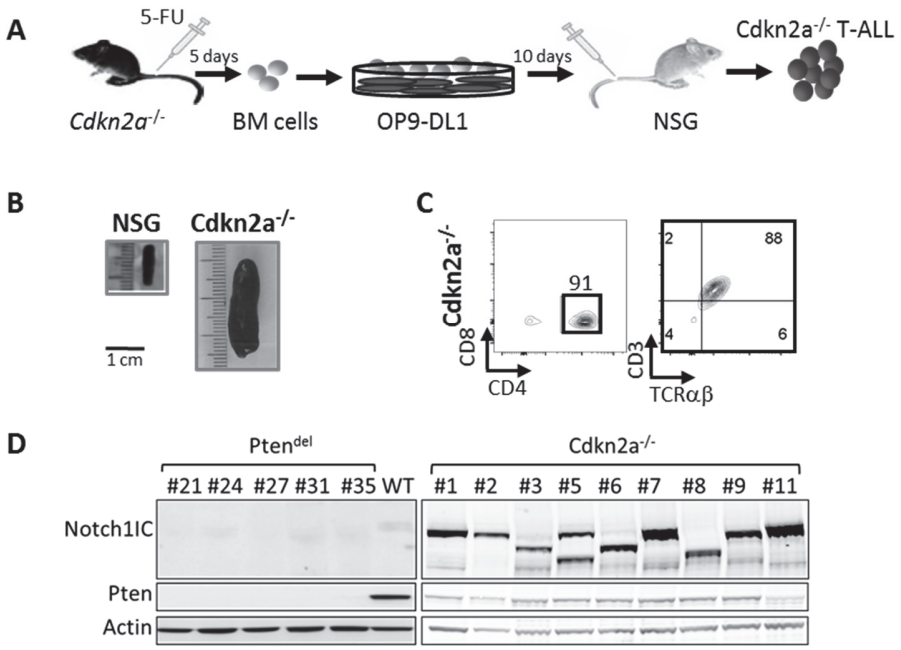

Supplementary figure S5: *Cdkn2a*$^{-/-}$ T-ALL mouse model. (A) Generation of *Cdkn2a*$^{-/-}$ T-ALL. Cells isolated from bone marrow of *Cdkn2a*$^{-/-}$ mice treated with 5-FU for 5 days were cultured on OP9-DL1 stroma for 10 days to engage cells toward T differentiation, before transplantation in NSG mice. Transplanted mice developed T-ALL in ~17 weeks, and 1.10^6 splenocytes of these mice can engraft NSG mice in less than 3 weeks. (**B**) Spleens from NSG mouse (left) and NSG mouse 3 weeks post-transplantation with *Cdkn2a*$^{-/-}$ T-ALL (right) (representative of n=9). (**C**) Flow cytometry analysis of a spleen from NSG mouse transplanted with *Cdkn2a*$^{-/-}$ T-ALL. CD4/CD8 expression (left) and CD3/TCRβ expression of the CD4 SP gate (right). Percentages of cells in the various gates are indicated. (**D**) Pten and activated Notch1 expression in T-ALL mouse models. Equivalent amounts of protein lysate from WT splenocytes, Pten^{del} and *Cdkn2a*$^{-/-}$ leukemic blasts were analyzed by immunoblotting with antibodies specific for cleaved Notch1, Pten and Actin as a loading control.

This T-ALL model deleted for *Cdkn2a* [4] (a tumor suppressor gene frequently mutated in human T-ALL) was used as a *Pten*-proficient control. In this model, referred to as *Cdkn2a*$^{-/-}$ T-ALL, all the tumors tested (n=9) were CD3/TCRαβ$^+$, monoclonal according to Vβ typing (supplementary Table S6), expressed Pten protein and were Notch1-IC activated, conversely to Pten^{del} T-ALL which are Notch1-independent as shown in panel **D**. Thus, while Pten^{del} and *Cdkn2a*$^{-/-}$ T-ALL recurrently gave rise to TCRαβ+ T-ALL, the oncogenic networks of both models are clearly distinct.

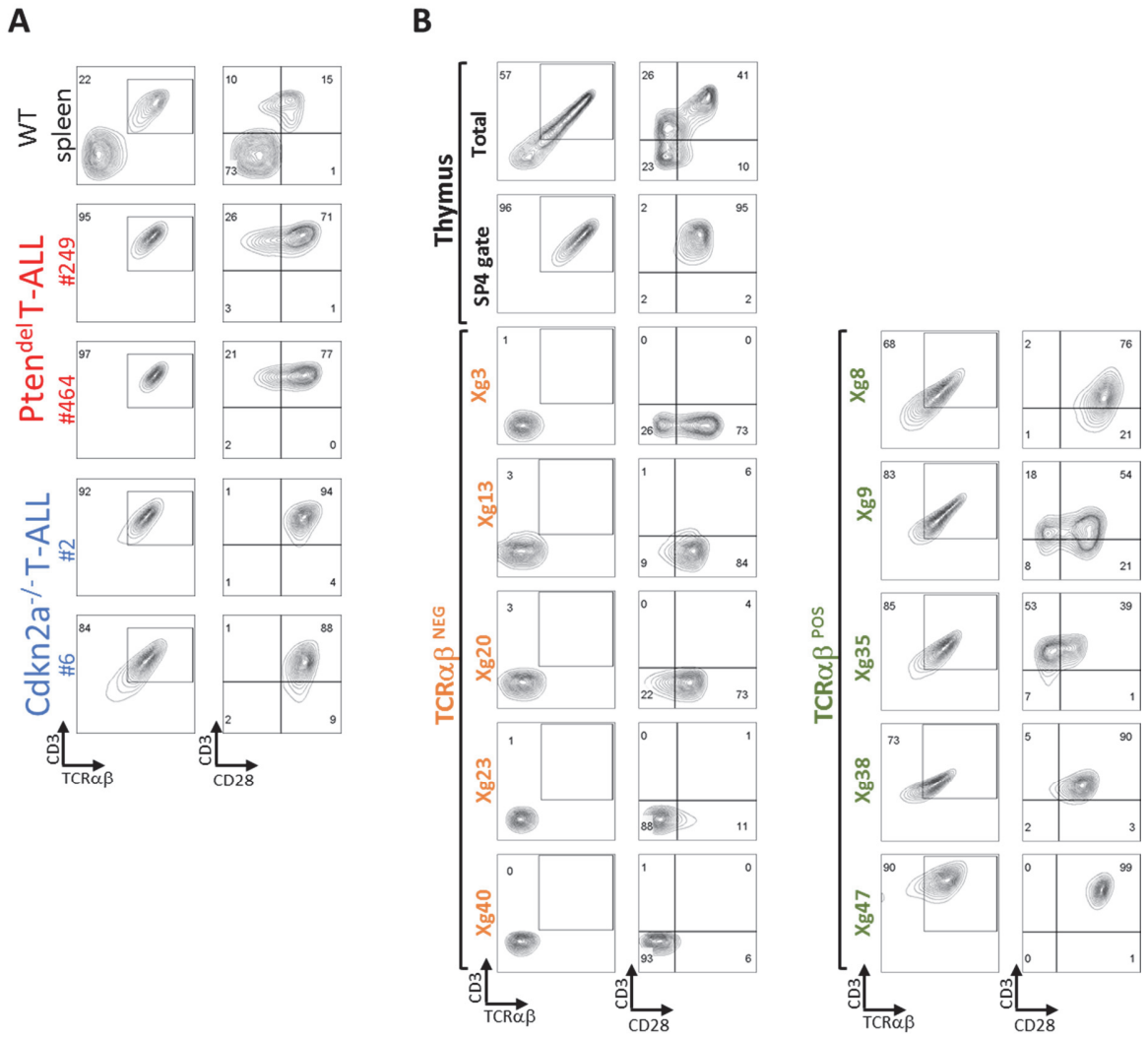

Supplementary Figure S6: Flow cytometry analysis of the expression of CD3 and TCRαβ (left) or CD3 and CD28 (right) in mouse T-ALL (A) and PDX samples (B). (**A**) 2 representative T-ALL from Pten^{del} and Cdkn2a$^{-/-}$ models are shown. WT control corresponds to C57BL/6 mouse. (**B**) Control corresponds to healthy human thymus: live cells without gate (total) and from SP4 gate were analyzed.

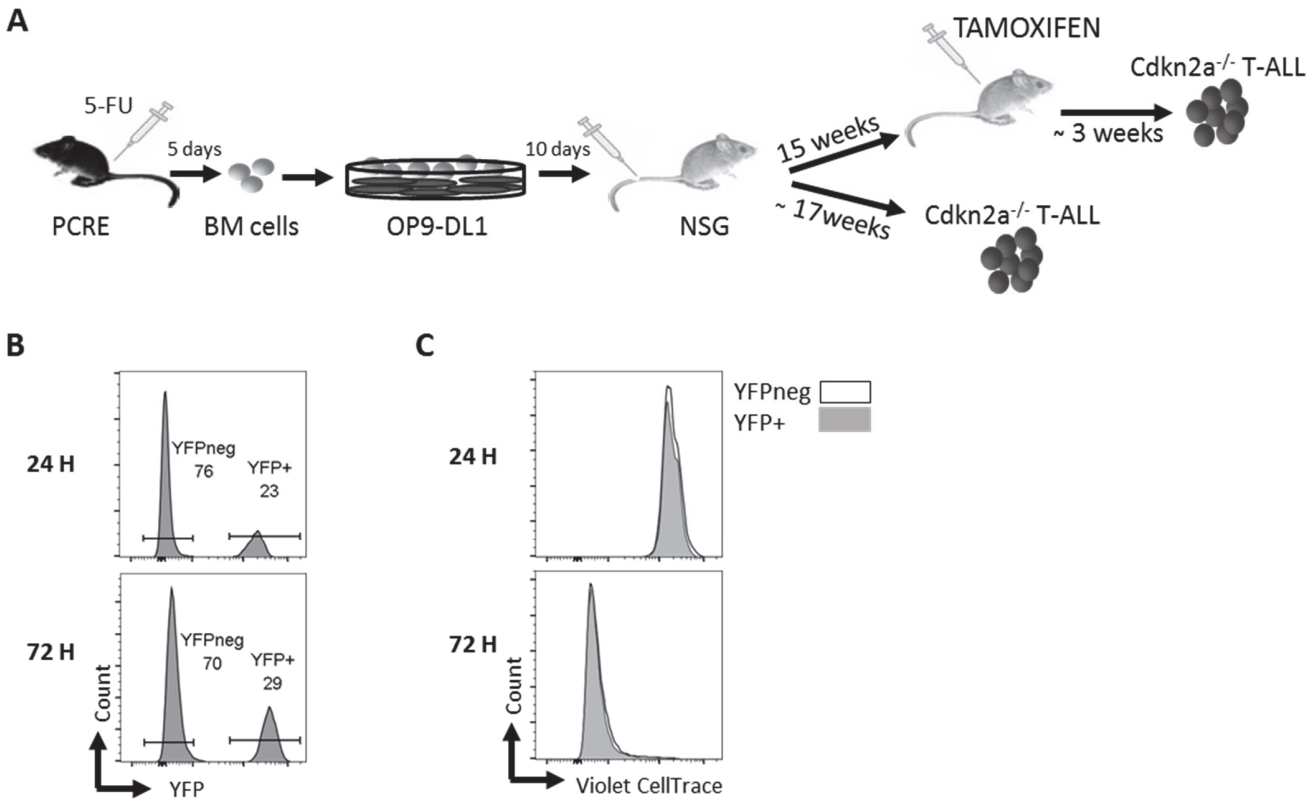

Supplementary Figure S7: **TCR stimulation-induced proliferation of TCR$\alpha\beta^+$ Cdkn2a$^{-/-}$ tumor cells is not decreased upon *Pten* deletion**. (**A**) PCRE tumors cells (Pten$^{fl/fl}$ Cdkn2a$^{-/-}$ RosaYFP CreERT2) were recovered after an *in vivo* treatment with Tamoxifen. Cells deleted for *Pten* are YFP positive whereas Pten^{pos} cells are YFP negative. To monitor cell proliferation, T-ALL were first labelled with Violet CellTrace reagent and then stimulated *in vitro* with anti-CD3/28 beads. 24 or 72H post-stimulation, cells were analyzed by flow cytometry; YFP (**B**) & CellTrace Violet (**C**) histograms are shown. We observed that anti-CD3/CD28 induced proliferation is similar for both YFP+ and YFP^{neg}, indicating that *Pten* deletion in established leukemic cells do not impede signaling.

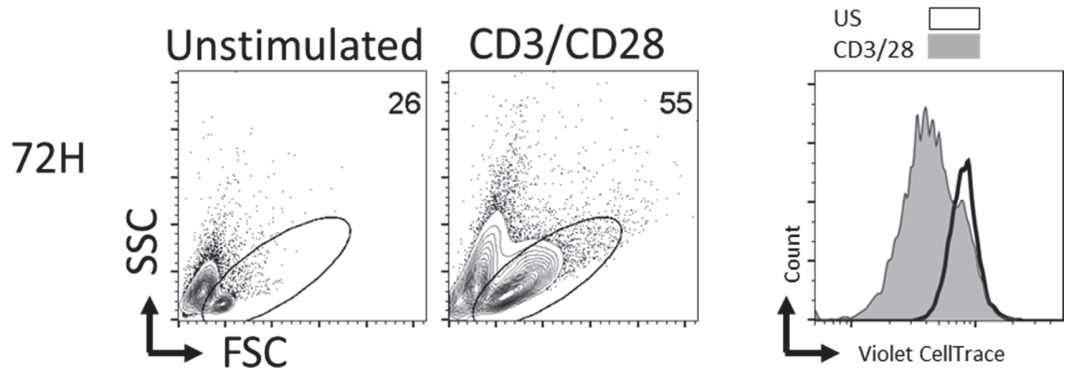

Supplementary Figure S8: ***Pten*** **deleted T-cells from disease-free mice respond to TCR triggering.** T-cells from spleen of 1 month-old disease-free Pten^{del} mouse were labelled with Violet cellTrace, cultured in absence (unstimulated, US) or in presence of anti-CD3/28 beads for 72H and then analyzed by flow cytometry. FSC/SSC contour plots (left) and CellTrace Violet (right) histograms are shown. We observed that conversely to unstimulated condition, stimulated Pten^{del} T-cells are proliferating (decrease of CellTrace Violet labeling).

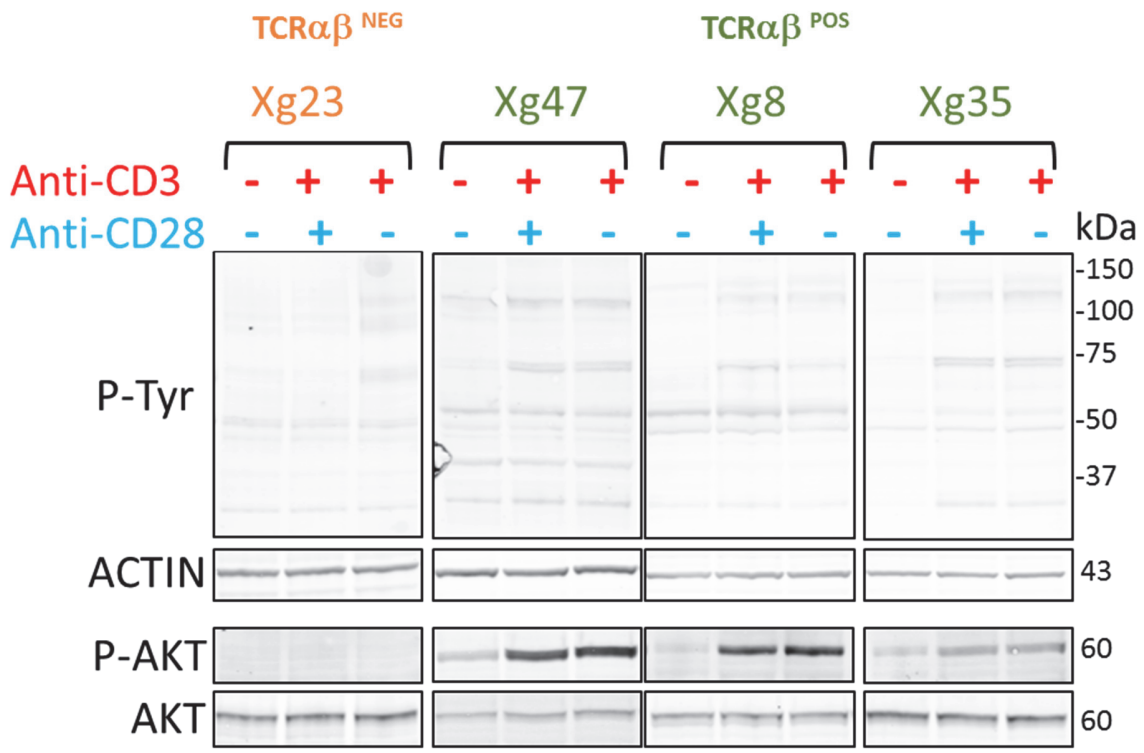

Supplementary Figure S9. TCR stimulation using anti-CD3/CD28 antibodies or anti-CD3 antibody only. PDX samples were untreated (-) or stimulated (+) with anti-CD3/CD28 antibodies or anti-CD3 antibody for 2 minutes and analyzed by immunoblotting with antibodies specific for phosphorylated tyrosine (P-TYR), phosphorylated S473 AKT (P-AKT), AKT and Actin.

In human T-ALL CD28 expression is heterogeneous. Thus, we tested anti-CD3 stimulation notably on Xg47 (TCRαβ^{high}/CD28^{high}), Xg8 (TCRαβ+/CD28+) and Xg35 (TCRαβ+/CD28-); as shown here, anti-CD3 and anti-CD3/28 stimulations gave rise to similar results (i.e. no noticeable increase of tyrosine phosphorylation and similar levels of P-AKT).

Supplementary Tables

Table S1. Oligonucleotide sequences

RQ-PCR Primers	Target	Sequence
Q-TCRb-S	Mouse OTII	tgtattcccatctctggacatctc
Q-TCRb-AS	Mouse OTII	agttcctgcccctgagtctgt
Q-ABL-S	Human Abelson	cttggccatttttggtttgg
Q-ABL-AS	Human Abelson	gccagtggagataacactctaagca
Q.ABL.HM-1S	Mouse Abelson	tgtggccagtggagataacactc
Q.ABL.HM-1AS	Mouse Abelson	ttcacaccattccccattgtg
Q-CD69-S	Human CD69	caagttcctgtcctgtgtgc
Q-CD69-AS	Human CD69	gagaatgtgtattggcctgga
Genotyping Primers		
CD4Cre-S	Cre	cgtacaccaaaatttgcct
CD4Cre-AS	Cre	agcattgctgtcacttggtcg
Pten-AS	Pten	ggcaaagaatcttggtgttac
Pten-S	Pten	gccttacctagtaaagcaag
Pten Ex4-S	Pten	gagagacattatgacaccgcc
Vb8.2 HY	HY1	ggctgcagtcacccaaagcccaag
Jb2-3 HY	HY2	cagtcagtctggttcctgagcc
Rag1 1746	RAG1	gaggttccgctacgactctg
Rag1 3104	RAG1	ccggacaagtttttcatcgt
Rag1 8162	RAG1	tggatgtggaatgtgtgcgag
Cre ERT2 wt-S	Cre ERT2	ctaggccacacagaattaaagatct
Cre ERT2 wt-AS	Cre ERT2	gtaggtggaaattctagcatcatcc
Cre ERT2 mutant-S	Cre ERT2	cgagtgatgaggttcgcaag
Cre ERT2 mutant-AS	Cre ERT2	tgagtgaacgaacctggtcg
OTII TCRa-S	TCRa OTII	aaagggagaaaaagctctcc
OTII TCRa-AS	TCRa OTII	acacagcaggttctgggttc
OTII TCRb-S	TCRb OTII	gctgctgcacagacctact
OTII TCRb-AS	TCRb OTII	cagctcacctaacacgagga
Rosa HL15	Rosa26-EYFP	aagaccgcgaagagtttgtcc
Rosa HL54	Rosa26-EYFP	taagcctgcccagaagactcc
Rosa HL152	Rosa26-EYFP	aagggagctgcagtggagta

Table S2: Antibodies used for immunoblotting

Primary antibody	Clone or reference	Company	Secondary antibody	Company
P-TYR	4G10	Millipore	CF680 anti-mouse	Interchim
pS473AKT	Ref :9271	Cell Signaling Technology	CF770 anti-rabbit	Interchim
AKT	Ref :9272	Cell Signaling Technology	CF770 anti-rabbit	Interchim
ACTIN	I-19	Santa Cruz Biotechnology	HRP anti-goat	Santa Cruz Biotechnology
PTEN	138G6	Cell Signaling Technology	HRP anti-rabbit	Santa Cruz Biotechnology
MYC	9-E10	Santa Cruz Biotechnology	HRP anti-mouse	Santa Cruz Biotechnology
Notch1IC	Val1744	Cell Signaling Technology	HRP anti-rabbit	Santa Cruz Biotechnology
BCL2	10C4	Santa Cruz Biotechnology	HRP anti-mouse	Santa Cruz Biotechnology

Table S3. Antibodies used for Flow Cytometry analysis of human cells.

Labeling	Conjugate	clone	company
CD1a	PE	NA1/34	Dako
CD3	V450	UCHT1	BD Pharmigen
CD3	APC	UCHT1	BD Pharmigen
CD4	V450	RPA-T4	BD Pharmigen
CD5	APC	UCHT2	BD Pharmigen
CD7	FITC	M-T701	BD Pharmigen
CD8	PercP Cy5.5	RPA-T8	BD Pharmigen
CD8	PE Cy7	RPA-T8	BD Pharmigen
CD8	PE	RPA-T8	BD Pharmigen
CD28	PE	CD28.2	BD Pharmigen
CD45	APC Cy7	2D1	BD Pharmigen
CD69	APC Cy7	FN50	BD Pharmigen
TCR αβ	PE Cy7	IP26	Biolegend

Table S4. Antibodies used for Flow Cytometry analysis of murine cells

Labeling	Conjugate	Clone	Company
CD3	APC Cy7	17A2	BD Pharmigen
CD4	V450	RM4-5	BD Pharmigen
CD4	APC	RM4-5	BD Pharmigen
CD5	APC	53-7.3	BD Pharmigen
CD5	FITC	53-7.3	BD Pharmigen
CD8	PercP	53-6.7	BD Pharmigen
CD8	PE	53-6.7	BD Pharmigen
CD25	PE	3C7	BD Pharmigen
CD28	FITC	E18	Biolegend
CD44	PE Cy7	IM7	Biolegend
CD44	APC	IM7	BD Pharmigen
CD45	PE	30F-11	BD Pharmigen
CD62L	APC	MEL-14	BD Pharmigen
CD69	PercP Cy 5.5	H1.2F3	BD Pharmigen
CD69	FITC	H1.2F3	BD Pharmigen
CCR9	FITC	eBioCW1.2	eBioscience
TCRβ	PE	H57-597	BD Pharmigen
TCRβ	APC	H57-597	BD Pharmigen
TCR Vβ5	FITC	MR9-4	BD Pharmigen
TCR Vα2	APC	B20.1	eBioscience
TCR HY	APC	T3.70	eBioscience

Table S5. Clonotyping of T-ALL developed by Pten^{del} mouse model

Mouse #	CD4/CD8	TCRαβ	clonality	TCRVβ
17	CD4+	+	Monoclonal	Vβ2
24	DN/CD4^{low}	+	Monoclonal	Vβ6
29	CD4+	+	Monoclonal	Vβ12
35	CD4+	+	Monoclonal	Vβ12
38	DP/CD4+	+	Monoclonal	Vβ16
63	DN	+	Oligoclonal	Vβ8.3 64%; Vβ14 31%
73	CD4+	+	Monoclonal	Vβ1
191	CD4+	+	Monoclonal	Vβ1
195	CD4+	+	Monoclonal	Vβ4
217	CD4+	+	Monoclonal	Vβ5
249	CD4+	+	Oligoclonal	Vβ6 85% ; Vβ5 15%
259	CD4+/DN	+	Monoclonal	Vβ7
260	CD4+	+	Oligoclonal	Vβ14 76% ; Vβ17 24%
267	CD8+/DN	+	Monoclonal	Vβ14
292	DN/CD4+	+	Monoclonal	Vβ11
464	CD4+	+	Monoclonal	Vβ20
470	DN/CD4+	+	Monoclonal	Vβ6
508	CD4+	+	Monoclonal	Vβ4

Table S6. Clonotyping of T-ALL developed by Cdkn2a$^{-/-}$ mouse model.

Tumor #	CD4/CD8	TCRαβ	clonality	TCRVβ	Pten protein
1	CD4+/CD8+	+	Monoclonal	Vβ7	+
2	DP/CD4+	+	Monoclonal	Vβ9	+
3	DP/CD4+	+	Monoclonal	Vβ7	+
5	CD4+	+	Monoclonal	Vβ7	+
6	CD4+	+	Monoclonal	Vβ6	+
7	DP/CD8+	+	Monoclonal	Vβ11	+
8	DP/CD8+	+	Monoclonal	Vβ5	+
9	CD4+	+	Monoclonal	Vβ 8.3	+
11	CD4+	+	Monoclonal	Vβ4	+

Table S7. Oncogenetic status of T-ALL samples used in this study. ND (not determined): T-ALL20 was screened and was found negative for BCR-ABL, SIL-TAL, AF4-MLL, TLX1, TLX3 & NUP214-ABL.

		Oncogenic status			PTEN Protein expression	Immunophenotype						
		NOTCH1	FBXW7	Others		CD1a	CD5	CD7	CD4	CD8	CD3	CD28
TCRαβ^{neg}	T-ALL 3	HD	GL	TLX3	+	+	+	+	+	-	-	+
	T-ALL 13	GL	GL	TAL1	+	-	+	+	+	+	-	low
	T-ALL 20	PEST	GL	ND	+	+	+	+	+dim	-	-	low
	T-ALL 23	GL	GL	TLX3	+	-	+	+	+	-	-	-
	T-ALL 40	PEST	GL	LYL1+	+	-	-	+	-	-	-	-
TCRαβ^{+}	T-ALL 8	GL	R465P	TAL1	-	-	+	+	+	-	+	+
	T-ALL 9	GL	GL	TAL1	-	-	+	+dim	-	-	+	+
	T-ALL 35	GL	GL	CALM AF10	-	+	+	+	-	-	+	low
	T-ALL 38	GL	GL	TAL1	-	-	+	+	-	-	+	+
	T-ALL 47	GL	GL	TAL1	-	-	+	+	-	-	+	+

Table S8. PTEN protein status in human TCRαβ^{+} T-ALLs

Reference	T-ALL	PTEN protein
Bonnet et al., Blood 2011[17]	12	NEG
	13	NEG
	15	NEG
	16	POS
	18	POS
	19	POS
	21	NEG
	23	LOW
	28R	NEG
	Xg	**PTEN protein**
This study	8	NEG
	9	NEG
	35	NEG
	37	POS
	38	NEG
	47	NEG

Supplementary References:

1. Marino, S. *et al.* PTEN is essential for cell migration but not for fate determination and tumourigenesis in the cerebellum. *Development* **129**, 3513-22 (2002).
2. Srinivas, S. *et al.* Cre reporter strains produced by targeted insertion of EYFP and ECFP into the ROSA26 locus. *BMC Dev Biol* **1**, 4 (2001).
3. Lee, P.P. *et al.* A critical role for Dnmt1 and DNA methylation in T cell development, function, and survival. *Immunity* **15**, 763-74 (2001).
4. Krimpenfort, P., Quon, K.C., Mooi, W.J., Loonstra, A. & Berns, A. Loss of p16Ink4a confers susceptibility to metastatic melanoma in mice. *Nature* **413**, 83-6 (2001).
5. Kisielow, P., Teh, H.S., Bluthmann, H. & von Boehmer, H. Positive selection of antigen-specific T cells in thymus by restricting MHC molecules. *Nature* **335**, 730-3 (1988).
6. Loosveld, M. *et al.* Therapeutic Targeting of c-Myc in T-Cell Acute Lymphoblastic Leukemia, T-ALL. *Oncotarget* **5**, 3168-72 (2014).
7. Asnafi, V. *et al.* Analysis of TCR, pT alpha, and RAG-1 in T-acute lymphoblastic leukemias improves understanding of early human T-lymphoid lineage commitment. *Blood* **101**, 2693-2703 (2003).
8. Ferrando, A.A. & Look, A.T. Gene expression profiling in T-cell acute lymphoblastic leukemia. *Semin.Hematol.* **40**, 274-280 (2003).
9. Soulier, J. *et al.* HOXA genes are included in genetic and biologic networks defining human acute T-cell leukemia (T-ALL). *Blood* **106**, 274-286 (2005).
10. Weng, A.P. *et al.* Activating mutations of NOTCH1 in human T cell acute lymphoblastic leukemia. *Science* **306**, 269-271 (2004).
11. Fasseu, M. *et al.* p16INK4A tumor suppressor gene expression and CD3epsilon deficiency but not pre-TCR deficiency inhibit TAL1-linked T-lineage leukemogenesis. *Blood* **110**, 2610-2619 (2007).
12. Guo, W. *et al.* Suppression of leukemia development caused by PTEN loss. *Proc Natl Acad Sci U S A* **108**, 1409-14 (2011).
13. Hagenbeek, T.J. *et al.* The loss of PTEN allows TCR alphabeta lineage thymocytes to bypass IL-7 and Pre-TCR-mediated signaling. *J Exp Med* **200**, 883-94 (2004).
14. von Boehmer, H. Unique features of the pre-T-cell receptor alpha-chain: not just a surrogate. *Nat Rev Immunol* **5**, 571-7 (2005).
15. von Boehmer, H. *et al.* Thymic selection revisited: how essential is it? *Immunol Rev* **191**, 62-78 (2003).
16. von Boehmer, H. & Kisielow, P. Negative selection of the T-cell repertoire: where and when does it occur? *Immunol Rev* **209**, 284-9 (2006).
17. Bonnet, M. *et al.* Posttranscriptional deregulation of MYC via PTEN constitutes a major alternative pathway of MYC activation in T-cell acute lymphoblastic leukemia. *Blood* **117**, 6650-9 (2011).